JOURNAL OF OPTOELECTRONICS AND ADVANCED MATERIALS, Vol. 9, No. 10, October 2007, p. 3285- 3292

Static and dynamic structure of liquid GaSb using the modified embedded atom method (MAEAM) potentials

S. SENTURK DALGIC*, U. DOMEKELI
Department of Physics, Trakya University, 22030, Edirne, Turkey

Using the effective potentials derived from the modified analytic Embedded Atom Method (MAEAM) in conjunction with the Variational Hypenetted Chain (VMHNC) liquid state theory, we have investigated the structure and atomic dynamics of liquid GaSb alloy near and above the melting point. The effective pair potentials have constructed from the MAEAM potential functions which are parameterized by fitting to both solid and liquid state properties of pure metals. The calculated partial pair correlation functions and static structure factors of liquid GaSb alloy near its melting have compared with experiment and the results of MD studies. The total structure factors of molten GaSb have computed at three different temperatures. The overall agreement has been found in reported works. The dynamical properties evaluated within the framework of the mode-coupling theory, using a self-consistent scheme have been also presented. The single-particle dynamics of the system has been analyzed by computing the mean square displacement (MSD) and velocity autocorrelation function (VACF). Temperature dependence of self diffusion coefficient and shear viscosity have also been shown. The collective dynamic properties such as the intermediate scattering function and the dynamic structure factor have determined.

(Received July 3, 2007; accepted October 1, 2007)

Keywords: Liquid GaSb alloy, Static and dynamic structural properties

1. Introduction

It is well known that III-V semiconductor compounds are important materials for electronic devices because of the many abnormal phenomena observed in their physical properties. The melting of the semiconductors such as Si, Ge, GaSb, InSb, etc. exhibits a special phenomenon, in which the covalent bond is destroyed and a semiconductor – metal transition occurs [1,2]. The GaSb is one of the popular III – V semiconductors that Zinc – blende – type GaSb crystalline phase is stable at ambient condition with a coordination number of 4. Upon melting, the GaSb becomes metallic, similar to Si and Ge, and transform to a more close – packed structure with density increasing, some of the covalent bonds are broken by the thermal motion of atoms, and the electronic states transform to delocalized or collective states in which compositional defects or "wrong" bonds exist (bonds between the same type of atoms are absent in the crystalline state) [3]. Despite the metallic behavior of GaSb in the melts, it retains some covalent properties [4]. To understand the mechanism of the transition and the origin of the property changes, the structural study of GaSb has attracted increasing attention in recent years [2-9].

One of the reported phenomena in physical properties of liquid GaSb is the abnormal changes observed in the temperature coefficient of resistivity (TCR) [8]. It has been noted that these changes of liquid-Sb-based alloys should be related to the peculiar local structure of Sb atoms in this liquid alloy. Another phenomenon reported in the literature is about the abnormal changes in viscosities of liquid GaSb, which were measured by Glazov et al. [4], Kakimoto and Hibiya [5] and Muziki et al. [2], show non-Arrhenius-type behavior. A non-Arrhenius relation means that there is not only one regime where the activation behavior can be observed. These experimental results suggest that the liquid structures of GaSb may change nontrivially with increasing temperature. Recently, Sato et al. [9] have measured the viscosities of liquid GaSb and found a good Arrhenius relationship in the temperature ranges of 991.9–1487.9 K. On the other hand Mizuki et al. have studied on the structure of molten state of GaSb [2] by neutron diffraction from 1073 to 1323 K, but no obvious changes of total structure factors and pair correlation functions were observed over this temperature range. Wang et al.[6] have also reported the studies on the structures of liquid GaSb by XAFS experimental method and the reverse Monte Carlo (RMC) simulation. On the theoretical side, Molteni et al. [10] have also calculated the liquid structure of GaSb with the tight-bonding molecular dynamics simulation. To gain more insight into the structural and dynamical properties and chemical bonding associated with liquid GaSb, Gu et. al. [3] have performed ab initio molecular-dynamics (AIMD) simulations based on density-functional theory (DFT) and the pseudopotential method [11], following the methods pioneered by Car and Parrinello [12]. In that work [3], they have first reported the partial structure factors and pair distribution functions of liquid GaSb.

According to our knowledge, there are no theoretical studies on the application of embedded atom method

(EAM) for liquid GaSb. In the present work, one of the version of EAM, namely the modified analytic embedded atom method (MAEAM) have first applied to investigate the static structure and atomic dynamic properties of liquid GaSb alloy using the integral equations. The original EAM which was proposed by Daw and Baskes (DB) [13] has been widely used in a wide range of metallic systems in many aspects of computer simulations, such as point defects alloying, segregation, surface, grain boundary structure and so on [14]. Based on Daw and Baskes' EAM model, Johnson had presented analytic EAM (AEAM) nearest-neighbor models for b.c.c , f.c.c , and h.c.p. metals and alloys [14]. Zhang et al. [15] developed a modified analytic EAM (MAEAM) model based on Johnson's (AEAM) model. Recently Fang et al. [16] have been constructed interatomic potentials for binary immiscible alloy systems with MAEAM, and then calculated the formation enthalpies for those systems. They have demonstrated that the MAEAM may be a reasonable method for immiscible alloys by comparing with other potential models [17]. In previous studies, it has been proved the MAEAM model can be explain successfully the structural properties of liquid K-Te, K-Sb and AsTe alloys [18-20]. This is motivated us to study for the liquid structure of GaSb alloy.

In this study, the recently proposed MAEAM based potential model [18] has been used to produce an effective pair potential which is capable of predicting the structural properties of liquid Ga, Sb metals and GaSb alloy. The parameters of the MAEAM potential functions are parameterized which give a good description of the liquid and still describe the solid accurately. One of purpose of the present paper is that to obtain the suitable effective interatomic pair potentials for binary liquid GaSb alloy based on the MAEAM. For this purpose, Finnis-Sinclair (FS) [21] type effective pair potential form of alloys based on the MAEAM which was proposed by Dalgic and co-workers have been used here [18, 19].

The presently obtained effective potentials for liquid GaSb alloy are used as input data in the structural and dynamic calculations. The partial static structure factors and pair distribution functions of this alloy have been performed with the variational modified hypernetted chain (VMHNC) liquid state theory [22] which was successfully applied to metallic systems in the EAM calculations [18,23-26]. The collective dynamic properties such as the intermediate scattering function and the dynamic structure factor have determined. The self diffusion coefficients and shear viscosities for liquid GaSb at different temperatures have been computed, and compared with the available results in literature.

2. Theory

2.1 Effective pair potentials

In the MAEAM model, the total internal energy of a system can be written as [15]:

$$E_{tot} = \sum F(\rho_i) + \frac{1}{2}\sum \phi(r_{ij}) + \sum M(P_i) \quad (1)$$

where $F(\rho_i)$ is the embedding function, $\phi(r_{ij})$ is the pair potential between atoms i and j with r_{ij} distance, $M(P_i)$ is the modification term and ρ_i is the electron density function induced at site i by all other atoms in the system which is given in the original form as

$$\rho_i = \sum f(r_{ij}). \quad (2)$$

The $M(P_i)$, $F(\rho_i)$ and atomic density function $f(r)$ in Eqs. (1, 2) are taken the forms as those used by Fang et al. [16]. The pair potentials in Eq.(1) can be given [16], as

$$\phi(r) = k_0 + k_{-1}\left(\frac{r}{r_{1e}}\right)^{-1} + k_1\left(\frac{r}{r_{1e}}\right) + k_2\left(\frac{r}{r_{1e}}\right)^2 + k_3\left(\frac{r}{r_{1e}}\right)^3 + k_4\left(\frac{r}{r_{1e}}\right)^4 + k_5\left(\frac{r}{r_{1e}}\right)^5 + k_6\left(\frac{r}{r_{1e}}\right)^6 \quad (3)$$

In the above equation, the fitting parameters are 8. In this work, we concentrate on the liquid state calculations. The potential functions have been parameterized with the method given in Ref. [18,23, 26].

In order to obtain the effective pair interactions of the MAEAM in the binary alloy, the recently proposed alloy effective potential form taken in Ref. [18] is used as:

$$\phi_{eff}^{AB}(r) = \phi_{AB}(r) - 2F'_{AB}(\rho) f_{AB}(r) M_{AB}(P_{AB}) \quad (4)$$

where the alloy pair potential $\phi^{AB}(r)$ between different atomic species is taken as:

$$\phi^{AB}(r) = \frac{1}{2}\left[\frac{f^B(r)}{f^A(r)}\phi^{AA}(r) + \frac{f^A(r)}{f^B(r)}\phi^{BB}(r)\right] \quad (5)$$

where AA and BB indicate A and B, type atoms in a binary alloy respectively. $\phi^{AA}(r)$ and $\phi^{BB}(r)$are the monatomic potentials given by Eqs. (3-4). In the above equations:

$$f_{AB}(r) = f_{e\,AB}\left(\frac{r_{1e\,AB}}{r}\right)^6 \quad (6)$$

where $r_{1eAB} = (r_{1eAA} + r_{1eBB})/2$, $f_{eAB} = (f_{eAA} + f_{eBB})/2$, The modification term of alloys can be given as

$$M_{AB}(P_{AB}) = \alpha_{AB}\left\{1 - exp\left[-\left(ln\left|\frac{P_{AB}}{P_{e\,AB}}\right|\right)^2\right]\right\} \quad (7)$$

where $\alpha_{AB} = (\alpha_{AA} + \alpha_{BB})/2$, $P_{eAB} = (P_{eAA} + P_{eBB})/2$, $P_{AB} = \sum_j f_{AB}^2(r_{ij})$.

2.2 Liquid State Theory

With the effective pair potential known, integral equations are able to provide us the liquid structure for metals. In our structural calculations, one of the integral equation theory which has shown to be very reliable theory of liquids is VMHNC has been carried out [26-28]. The well known Ornstein-Zernike (OZ) equation, which for a homogeneous, isotropic, binary system reads (i, j =1, 2) can be written as

$$h_{ij}(r) = c_{ij}(r) + \sum_{l=1}^{2} \rho_l h_{il}(r) * c_{lj}(r) \qquad (8)$$

which defines the partial direct correlation functions, $c_{ij}(r)$, in terms of the total correlation functions $h_{ij}(r)=g_{ij}(r)-1$, where $g_{ij}(r)$ denote the partial pair distribution functions and ρ_l denote the partial ionic number densities. Eq.(8) is supplemented by the exact closure relation of MHNC in terms of $\phi^{AB}_{eff}(r)$are the interatomic pair potentials and the $B_{ij}(r)$ PY bridge functions for binary system. In the present work, we have carried out the VMHNC integral equation theory which was extended by Gonzalez et al. [28] so as to minimize the configurational Helmholtz free energy functional $f^{VMHNC}(\beta,\rho,x_l,\eta_\alpha)$ by the variational condition. The total structure factor and the total pair correlation function for liquid alloy are calculated using the expression as a linear combination of partial structure factors $S_{ij}(q)$ [18] and partial pair correlation functions $g_{ij}(r)$ with the neutron scattering amplitudes which are taken from [3].

2.3 Dynamic properties

The self –diffusion coefficient D_i of the i species in the liquid alloy can be calculated using time – dependent correlation functions [29] known as the Einstein (E) relation in which the coefficient is given as the time integral of a corresponding time correlation function.

$$D_i = \lim_{t\to\infty} \frac{\langle \Delta r_i(t)^2 \rangle}{6t} \qquad (9)$$

where $< \Delta r_i(t)^2 >$ defined as the mean square displacement (MSD) of a tagged particle. Also the self diffusion coefficient D_i can be computed by the Green – Kubo (GK) relation as

$$D_i = \frac{k_B T}{m} \int_0^\infty Z_i(t)\, dt \qquad (10)$$

where $Z_i(t)$ is the velocity autocorrelation function (VACF) defined as single particle correlation

$$Z_i(t) = \frac{\langle v_{i1}(t) v_{i1}(0) \rangle}{\langle v_{i1}^2 \rangle} \qquad (11)$$

In this work, the diffusivity for each constituent in the alloy has been found using the theory for the dynamic structure calculations given in Refs. [30,31] for details. The viscosity η is given as in Ref. [3]:

$$\eta = \frac{k_B T}{2\pi a D} \qquad (12)$$

where $D=(D_{Ga}+D_{Sb})/2$ [3], a is the effective diameter of the diffusing particles. We define the size a as the average value of the nearest – neighbor distances of each species in the liquid alloy. Finally, The collective dynamical properties in GaSb are embodied in three partial dynamic structure factors, namely $S_{GaGa}(q,w)$, $S_{GaSb}(q,w)$, $S_{SbSb}(q,w)$ which can be obtained by a time Fourier transform of the $F_{GaGa}(q,w)$, $F_{GaSb}(q,w)$, $F_{SbSb}(q,w)$..

$$S_{GaSb}(q,w) = \frac{1}{2\pi} \int dt\, F_{GaSb}(\vec{q},t)\, e^{iwt} \qquad (13)$$

where $F_{GaSb}(q,w)$ is the intermediate scattering function of GaSb in liquid $Ga_{0.5}\,Sb_{0.5}$ alloy.

3. Results and discussion

3.1 Effective Pair Potentials

The input parameters, such as the ionic number densities and thermodynamic states for pure liquids Ga and Sb are taken from Waseda [32] and given in Table 1 where s and l indicate the solid and liquid phases, respectively. The solid state values in Table 1 are taken from Kittel [33].

Table 1. The input data used in our calculations.

Metal	T(K)	ρ(at./A^3)	E_c^s (eV)	E_c^l (eV)	a^s (A)	a^l (A)
Ga	1073	0.0484	2.81	2.79	3.56	3.62
Sb	933	0.0320	2.75	2.74	3.74	3.78

In this work for the purpose of the liquid state calculations, we have used the Rose's equation of state (EOS) [34] in order to calculate the cohesive energy for pure metals at given temperature. We have determined the parameters of the potential functions by combining the two equations for the cut off procedure and the equation of the equilibrium condition, the equation for the cohesive energy; the equation for minimizing the configurational free energy

(details are given in Ref. [18,19]). The model parameters for Ga and Sb obtained from the presented procedure are listed in Table 2.

Table 2. The MAEAM potential parameters for Ga and Sb.

Ga		Sb	
Parameters	Values	Parameters	Values
n	0.830000	n	0.820000
F_0(ev)	1.866481	F_0(ev)	1.832516
α (ev)	0.278600	α (ev)	0.321076
k_{-1}(ev)	69.76654	k_{-1}(ev)	60.71935
k_0(ev)	-306.8724	k_0(ev)	-267.0778
k_1(ev)	571.6117	k_1(ev)	497.4863
k_2(ev)	-588.0956	k_2(ev)	-511.8326
k_3(ev)	362.1252	k_3(ev)	315.1655
k_4(ev)	-133.6498	k_4(ev)	-116.3184
k_5(ev)	27.38275	k_5(ev)	23.83181
k_6(ev)	-2.401664	k_6(ev)	-2.090221
r_c(A)	5.125000	r_c(A)	5.425000

The constructed MAEAM effective pair potentials for liquids Ga and Sb are used as input data in our VMHNC calculations. We have extended the Fang' MAEAM in order to obtain structural properties of the liquid equiatomic GaSb. The resultant FS type alloy effective potentials are shown in Fig 1.

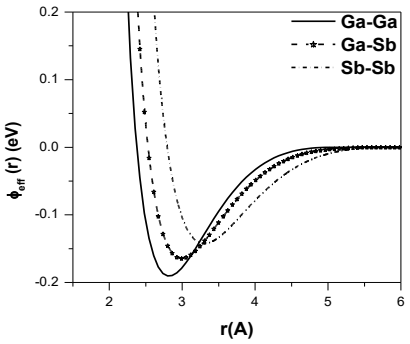

Fig. 1. MAEAM effective pair potentials for liquid GaSb alloy.

The partial pair potentials of liquid GaSb give the correct trends as far as the position of the concerned. As we go from Ga to Sb in periodic table, the calculated potentials become flatter and the width increases.

3.2 Structural Properties

As described in the preceding section, the effective potentials are used as input data in our structural calculations. We have obtained the static and dynamic structure properties of liquid GaSb alloy at thermodynamic states ρ =6.733-6.668x$10^{-4}T$ (ρ in 10^3kg m^{-3}) [9] for a temperature range of 991 – 1487 K. The pair distribution functions, g(r), obtained from the VMHNC calculations are shown in Fig. 2, which also shows the corresponding experimental data measured by x-ray diffraction experiments [32] and ab initio MD results [3].

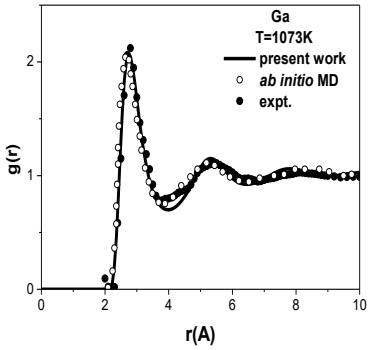

a

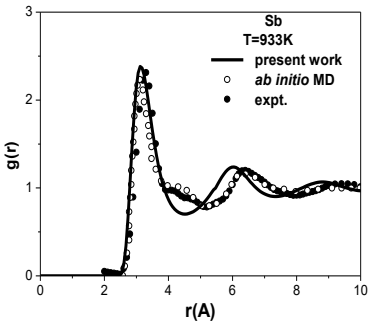

b

Fig. 2. Pair distribution functions for liquids (a) Ga and (b) Sb .

There is an agreement between the calculated VMHNC results and experimental data for liquid Ga. The VMHNC result of Sb shows a major difference in the region 4 < r <10 with the x-ray and MD results. In Fig. 3, we have presented the calculated VMHNC partial distribution functions for Ga-Ga, Sb-Sb and Ga-Sb in liquid GaSb alloy by comparing with ab initio MD results of Gu et. al.[3].

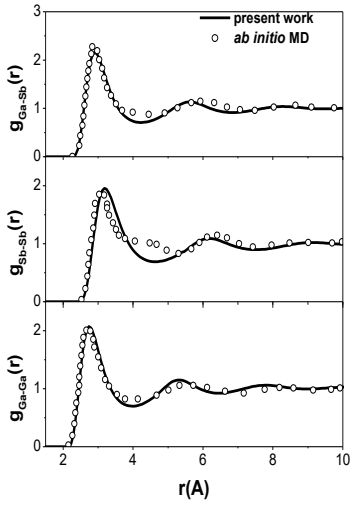

Fig. 3. Partial pair distribution functions for liquid alloy GaSb at 1073 K.

The present results for partial pair distribution functions are well predicted as the position and height of the first peak of ab initio MD results for $g_{Ga\text{-}Ga}(r)$, $g_{Ga\text{-}Sb}(r)$ and $g_{Sb\text{-}Sb}(r)$. We note that a particular feature seen in the first minima of $g_{Sb\text{-}Sb}(r)$ obtained by ab initio MD can not occur for VMHNC. Our results for $g_{Sb\text{-}Sb}(r)$ show that Sb has a liquid character in this alloy composition. Fig. 4 shows the total structure factors, S(q), obtained by the VMHNC theory at three different thermodynamic states as 1073, 1173 and 1323 K. We have compared our results with experimental data given by Mizuki *et.al.* [2]. In Fig.4, it is also been displayed together with ab initio MD [3] for 1073K.

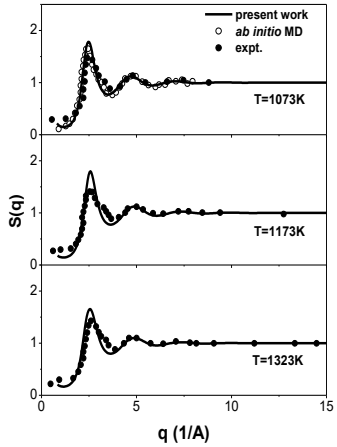

Fig. 4. The total structure factors for liquid GaSb alloy at 1073, 1173 and 1323 K.

It appears in Fig.4 that the first peak of the calculated total structure factor is overestimated than experimental data but agree well with ab initio MD results at 1073 K. Also, there are small differences between the phase of oscillations of experimental and our calculated results at every temperature. The VMHNC results damped oscillations than experimental results the studied alloy composition at 1073, 1173 and 1323K. The total pair correlation function of liquid GaSb obtained by weighting the partial pair correlation functions with the neutron scattering lengths is shown in Fig. 5.

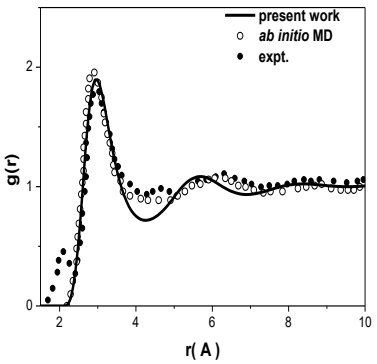

Fig. 5 The total pair correlation functions for liquid GaSb alloy at 1073K.

The total pair correlation function obtained by the VMHNC theory is in a good agreement with the ab initio MD [3] and the experimental result [2], except the intermediate r range which is concerned with the partial correlation function of $g_{SbSb}(r)$. Gu et al. [3] has been noted that the small peak in g(r) around 2 A in observed data is artificial, arising from the limited q range of the experimental structure factor of Muziki et al. [2] (the experimental pair correlation function is calculated from structure factor S(q) by Fourier transform). It is possible to estimate coordination number from the total g(r) as in Ref. [5] $N = 2\int_0^{r_{max}} 4\pi r^2 \rho\, g(r)dr$, where r_{max} is the position of the first peak in radial distribution function. (for liquid GaSb, r_{max} = 2.98 A). We find N=5.9 for liquid GaSb and its corresponding experimental and ab initio MD values are 5.4±0.5 and 5.5, respectively [2,3].

3.3 Dynamic Properties

In order to discuss time dependent properties of liquid GaSb alloy, the result of the normalized velocity autocorrelation function and mean square displacement are plotted in Fig. 6a,b for Ga and Sb in liquid GaSb alloy at 1073 K, respectively. We can compare our results of $Z(t)$ and $<\Delta r^2(t)>$ with those obtained with ab initio MD [3].

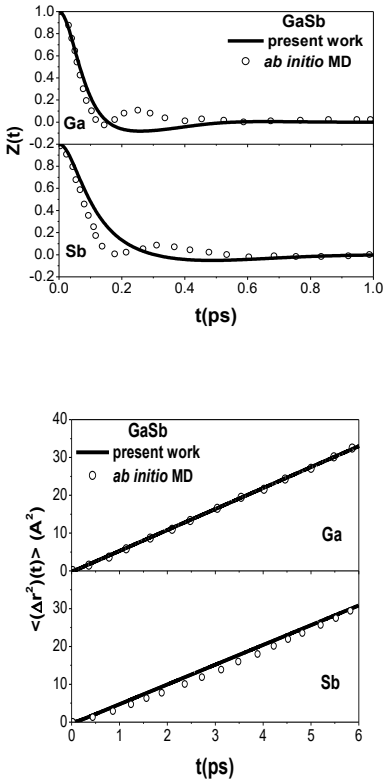

Fig. 6. (a) The normalized velocity autocorrelation functions and (b) mean square displacements for Ga and Sb in liquid GaSb alloy at 1073 K

In all cases, in Fig. 6a, Z(t) becomes negative which is known as a famous cage effect due to temporary trapping of particles by their neighbours, and subsequently shows decay without any oscillations in contrast with the molten alkali and alkali – earth metals [31]. It is clearly relevant for the magnitude of the self – diffusion coefficient (proportional to the area under Z(t) and it affects Z(t) in a short time regime. In Fig. 6b, the calculated mean square displacements are in good agreement with ab initio MD results for Ga and Sb in liquid GaSb alloy at 1073 K. However it is possible to say, time dependence of the mean square displacement shows typical behaviour for simple liquids at higher temperatures. For longer times, as soon as the motions become diffusive, the mean square displacement has a linear dependence on time.

The results obtained for the self – diffusion coefficients and shear viscosity are shown in Table 3 for liquid GaSb compared with both experimental data [9] and ab initio MD results [3]. The values of the self – diffusion coefficients obtained in this work using the corresponding GK and E relations are mutually consistent.

The calculated self – diffusion coefficients are in good agreement with ab initio MD results for Ga and Sb in liquid GaSb alloy at 1073 K. In this work, the values of the shear viscosity computed by Eq.(12). The calculated viscosity of liquid GaSb at 1073K is in good agreement the experimental data.

The intermediate scattering function is concerned with density of fluctuations over both the length and time scales. In Fig. 7a shows the results for normalized intermediate scattering functions obtained from the present MAEAM model for different q values namely, $2q_p/9$, $2q_p/5$, $2q_p/3$, and q_p, where q_p is the position of the first peak in partial structure factor. (for liquid Ga-Sb, q_p =2.47 A^{-1}).

Table 3. The calculated self – diffusion coefficients for Ga and Sb in liquid GaSb alloy, and shear viscosity for liquid GaSb alloy. Values in parentheses show the diffusion coefficients and viscosity obtained from ab initio MD [3].

T(K)	D(A^2/ps)				η(mPa s)	
	GK		E			
	Ga	Sb	Ga	Sb	GaSb	Expt.
1073	0.932(0.939)	0.876 (0.856)	0.924 (0.932)	0.862 (0.872)	0.879(0.900)	0.870[a]

[a] The experimental results from Ref. [9]

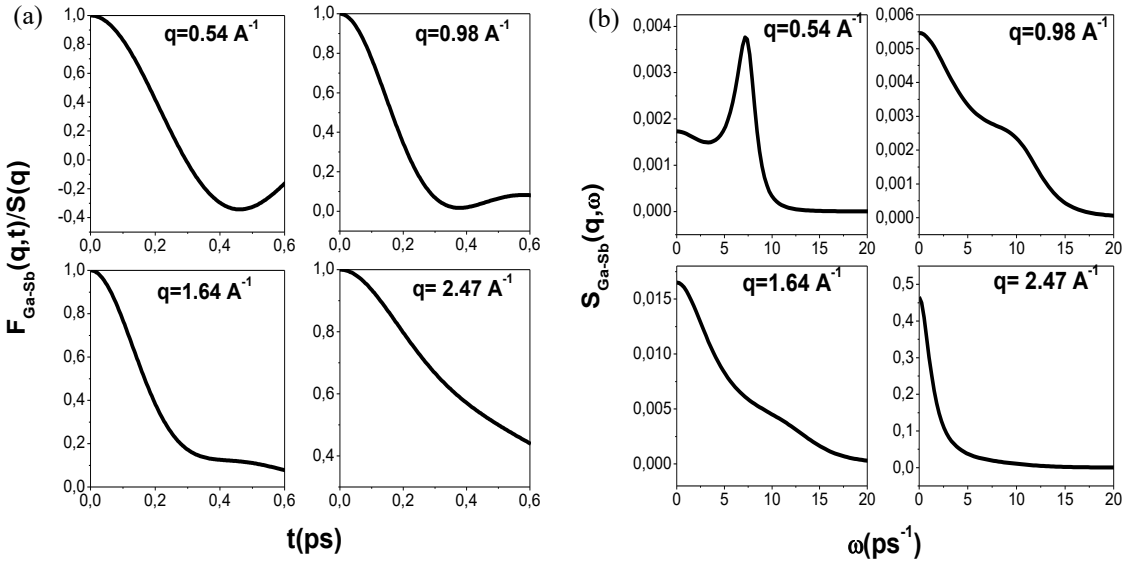

Fig. 7(a). The intermediate scattering function and (b) the dynamic structure factor for Ga-Sb in liquid GaSb alloy at 1073 K.

In Fig. 7a, the most significant feature of $F_{GaSb}(q,t)$ is the pronounced oscillations observed at low q. The intermediate scattering function exhibits an oscillatory behaviour which persists up to $q \approx 2q_p/3$, with the amplitude of oscillations beging stronger for the smaller q values. This is typical behavior found for other simple liquid metals near melting. It is well known that $F_{GASb}(q,t)$ is closely connected to the dynamic structure factor $S_{GaSb}(q,w)$, which is obtained by a time Fourier transform of the $F_{GaSb}(q,t)$. Our results for $S_{GaSb}(q,w)$ shown in Fig. 7b reveal two main feature: a peak centered at zero frequency representing decaying fluctuations and a finite – frequency peak representing oscillations. The dynamic structure factor shows weak side peaks, indicative of

collective density excitations up to $q \approx 1.64$ A^{-1}. The strongly diffusive character of the F(q,t)' s obtained from the VMHNC calculations, give rice to S(q,w) which decay rather quickly.

In order to determine the time dependence of self – diffusion coefficient, the results for the self – diffusion coefficients are plotted versus inverse temperature for Ga and Sb in liquid GaSb alloy in Fig 8. The self – diffusion coefficient of liquid GaSb alloy has been calculated at temperatures above melting point, i. e. in the liquid state. These calculations are limited within a temperature range of 991 – 1487 K. From Fig. 8, it is found that the diffusiun of the liquid Ga and Sb in GaSb alloy exhibits Arrhenius type behaviour. In all calculated results, *D* of Ga is larger than that of Sb. We know that self – diffusion coefficients are sensitive to the change of liquid structure and can be served as another way to study the microstructure of liquid. Obviously, the difference between the self – diffusion coefficients of Ga and Sb rises with increasing temperature because the mass of Ga atom is smaller than that of Sb atom.

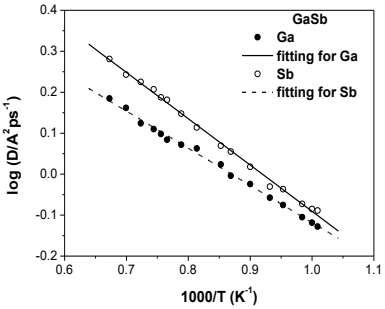

Fig.8. The calculated self-diffusion coefficients of liquid GaSb alloy.

Logarithmic representation displayed in the Arrhenius – type diagram, with viscosity as a function of 1000/T for liquid GaSb is given in Fig 9. We compare our results of viscosity with values given in Ref. [2,4,5,9] in the same figure.

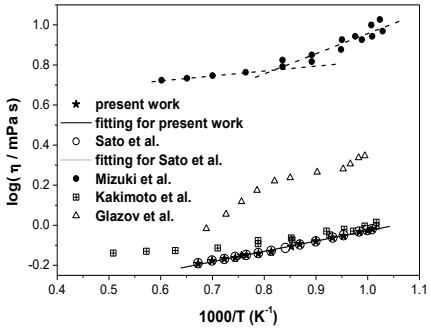

Fig 9. The viscosities for liquid GaSb as a function of inverse temperature.

The calculated viscosities for liquid GaSb are in good agreement with the values of Sato et al. [9] and smaller than those of Glazov et al.[4], Kakimoto et al. [5] and Mizuki et al. [2]. Also, we have shown that the shear viscosity of liquid GaSb exhibit Arrhenius type behavior in the temperature range 991 – 1487 K as Sato et.al [9] obtained.

4. Conclusions

The presented MAEAM provides a realistic description of the pair interaction in liquid GaSb alloy. We have used the recently improved the functional forms of the effective pair potentials for MAEAM to obtain a good description of the liquid and still describe the solid accurately. We note that our effective pair potentials show long-range character different from other MAEAM derived potentials for solids. The structural calculations were carried out using MAEAM derived effective pair potentials with the VMHNC theory of liquids. Comparison between the results of the VMHNC theory and available experimental and ab initio MD results show that the proposed MAEAM formalism for, GaSb alloy systems is capable of providing a good description in their liquid state. The dynamical properties of liquid GaSb alloy evaluated within the framework of the mode-coupling theory, using a self-consistent scheme have been also presented. The single-particle dynamics of the system has been analyzed by computing several time correlation functions. Temperature dependence on the self diffusion coefficient and the shear viscosity for liquid GaSb alloy are reported. The calculated results for these transport properties seem to exhibit Arrhenius behavior. The computed values of self diffusion coefficient and shear viscosity are consistent with available results in literature. These results suggest that pair potentials constructed on the basis of MAEAM may also be capable of describing other single particle and collective dynamics properties of liquid semiconductors, such as intermediate scattering function. In addition to this these potentials may be useful in theoretical dynamic properties of liquid semiconductors and alloys.

Acknowledgements

This work is supported from the Research Foundation of Trakya University under Project Number TUBAP 780.

References

[1] M. Tosi, J. Phys.: Condens. Matter **6**, A13 (1993).
[2] J. Mizuki, K. Kakimoto, M. Misawa, T. Ukunaga, N. Watanabe, J. Phys.: Condens. Matter **5**, 3391 (1993).
[3] T. Gu, X. Bian, J. Qin, C. Xu, Phys. Rev. **B 71**, 104206 (2005).
[4] V. M. Glazov, S. N. Chizhevskaya, and N. N. Glagoleva, Liquid Semiconductors Plenum, New York (1969).

[5] K. Kakimoto T. Hibiya, J. Appl. Phys. **66**, 4181 (1989).
[6] Y. R. Wang, K. Q. Lu, and C. X. Li, Phys. Rev. Lett. **79**, 3664 (1997).
[7] K. Lu, Q. Wang, C. Li, Y. Wang, X. Chen, J. Non-Cryst Solids **312-314**, 34 (2002).
[8] Q. Wang, X. M. Chen, and K. Q. Lu, J. Phys.: Condens. Matter **12**, 5201 (2000).
[9] Y. Sato, T. Nishizuka, T. Takamizawa, T. Yamamura, Y. Waseda, Int. J. Thermophys. **23**, 235 (2002).
[10] C. Monlteni, L. Colombo and L. Miglio, J. Phys. Condens. Matter **6**, 5255 (1994).
[11] R. O. Jones, O. Gunnarsson, Rev. Mod. Phys. **61**, 689 (1989).
[12] R. Car, M. Parrinello, Phys. Rev. Lett. **55**, 2471(1985).
[13] M. S. Daw, M. I. Baskes, Phys. Rev. Lett. **50**, 1285 (1983).
[14] R. A.Johnson, D. J. Oh, J. Mater. Res. **4**, 1195 (1989); R. A. Jonhson, J. Mater. Res. **3**, 471(1988).
[15] B. W. Zhang, Y. F. Ouyang, Phys. Rev. **B 48**, 3022 (1993).
[16] F. Fang, X. L. Shu, H. Q. Deng, W. Y. Hu, M. Zhu, Mater. Sci. and Eng. **A 355**, 357 (2003).
[17] Y. F. Ouyang, B. W. Zhang, S. Z. Liao, Z. P. Jin, Z. Phys. **B 101**, 161 (1996).
[18] G. Tezgor, S. S. Dalgic, U. Domekeli, J. Optoelectron. Adv. Mater. **7**, 1983 (2005).
[19] S. S. Dalgic and U. Domekeli, J. Optoelectron. Adv. Mater. **9**, 1705 (2007).
[20] S. S. Dalgic, S. Sengul, J. Optoelectron. Adv. Mater. **9**, 1699 (2007).
[21] M. W. Finnis, J.E. Sinclair, Phil. Mag. **A 50**, 45 (1984).
[22] L. E. Gonzalez, D. J. Gonzalez and M. Silbert, Phys. Rev. **A 45**, 3803 (1992); L. E. Gonzalez, M. Silbert, D. J. Gonzalez, S. Dalgic, Z. Phys. **B 103**, 13 (1997).
[23] S. S. Dalgic, S. Dalgic, U. Domekeli, J. Optoelectron. Adv. Mater. **5**, 1263 (2003).
[24] G. M. Bhuiyan, M. Silbert and M. J. Stott, Phys. Rev. **B 53**, 636 (1995).
[25] M. M. G. Alemany, M. Calleja, C. Rey, L. J. Gallego, J. Casas, L. E. Gonzalez, J. Non-Cryst Solids **250-252**, 53 (1999).
[26] S. Senturk. Dalgic, S. Sengul, S. Kalaycı, J. Optoelectron. Adv. Mater. **7**, 2001 (2005).
[27] H. Kes, S. S. Dalgıc, S. Dalgıc and G. Tezgor, J. Optoelectron. Adv. Mater. **5**, 1281 (2003).
[28] L. E. Gonzalez, A. Meyer, M. P. Iniguez, D. J. Gonzalez, M. Silbert, Phys. Rev **E47**, 4120 (1993).
[29] J. P. Hansen and I. R. McDonald, Theory of Simple Liquids, Academic Press, London (1986).
[30] M. M. Alemany, J. Casas, C. Rey, L. E. Gonzalez, L. J. Gallego, Phys. Rev **E56**, 6818 (1997).
[31] S. Dalgic, M. Colakogullari, S. Senturk Dalgic, J. Optoelectron. Adv. Mater. **7**, 1993 (2005).
[32] Y. Waseda, The Structure of Non – Crystalline Materials, McGraw – Hill , New York (1981).
[34] C. Kittel, Introduction to Solid State Physics, 6 th edition (1986).
[35] J. H. Rose, J. R. Smith, F. Guinea, J. Ferrante, Phys. Rev. **B 29**, 2963 (1984).

*Corresponding author: serapd@trakya.edu.tr